Available online at www.sciencedirect.com
ScienceDirect
Mendeleev Commun., 2024, **34**, 584–586

Mendeleev Communications

4-Phenyldiazenyl-substituted 3,6-di-*tert*-butylcatechol: synthesis and azo–hydrazone equilibrium

**Konstantin A. Martyanov, Arina A. Tsybushkina, Anton V. Cherkasov,
Alexey A. Belikov and Viacheslav A. Kuropatov***

*G. A. Razuvaev Institute of Organometallic Chemistry, Russian Academy of Sciences,
603950 Nizhny Novgorod, Russian Federation. E-mail: viach@iomc.ras.ru*

DOI: 10.1016/j.mencom.2024.06.038

Reaction of 3-hydroxy-2,5-di-*tert*-butyl-1,4-benzoquinone with phenylhydrazine hydrochloride mainly leads to the corresponding hydrazone at the position 1 existing in tautomeric equilibrium with 3,6-di-*tert*-butyl-4-(phenyldiazenyl)catechol. Thermodynamic parameters of the tautomerization were evaluated by NMR spectroscopy. The hydrazone structure was confirmed by XRD study.

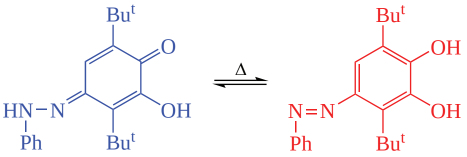

Keywords: dioxolene ligands, photoresponsive ligands, benzoquinones, *p*-iminoquinone, azo compounds, hydrazones, azo–hydrazone tautomerism.

Design of molecular switches is considered to be a research area of high relevance and practical importance.[1–4] The key feature of molecular switches is their ability to undergo a reversible transition between two (or more) stable forms responding to external stimuli, such as temperature, irradiation, pH of medium, pressure, *etc*. Various types of compounds have been successfully applied as molecular switches. For example, azobenzene derivatives are known as a large class of organic photoswitches due to their ability for reversible *E*–*Z* isomerization under light irradiation.[5–9] Also, the phenomenon of magnetic bistability is observed for dioxolene metal complexes exhibiting thermally-induced valence tautomerism[10–13] and spin crossover.[14,15]

An idea to combine the above-mentioned azo group and dioxolene metal complex in one molecule seems promising in searching for ligand-driven light-induced effects of magnetic switching, such as LD-LISC[16,17] and LD-CISSS.[18,19] Previously, some synthetic procedures for the preparation of azo-containing catechols by the azo-coupling of catechols with arenediazonium substrates have been reported.[20,21] Alternatively, preparation of azo-containing phenols may be accomplished *via* the reaction of 1,4-benzoquinones with arylhydrazines.[22] Thus, in order to obtain the corresponding phenyldiazenyl-substituted 3,6-di-*tert*-butylcatechol, 2,5-di-*tert*-butyl-3-hydroxy-1,4-benzoquinone **1** may be used as starting material. Indeed, the reaction of **1** with phenylhydrazine hydrochloride afforded hydrazone derivative **2** being a prototropic tautomer of azo catechol (Scheme 1).

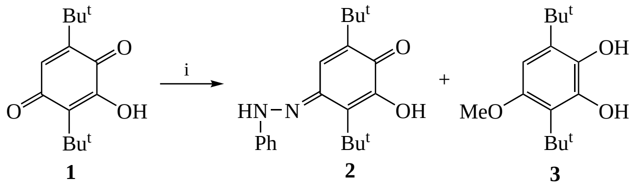

Scheme 1 *Reagents and conditions*: i, $N_2H_4 \cdot HCl$ (1 equiv.), MeOH, reflux, 48 h.

p-Iminoquinone **2** was isolated with 43% preparative yield. The imination proceeds regioselectively at one carbonyl group: the formation of bis-hydrazone product was not observed even if double excess of phenylhydrazine was used. Methanol was found to be the most appropriate solvent for the reaction, whereas in acetonitrile, toluene or chloroform only traces of the desired product were detected. At the same time, it should be mentioned that **2** is not the only product of the reaction: after isolation of **2**, slow cooling of mother liquor resulted in precipitation of known[23] 4-methoxy-3,6-di-*tert*-butylcatechol **3** that was isolated with 18% preparative yield. The reason for formation of **3** is in dual nucleophile and reductant nature of phenylhydrazine.

Single crystals of **2** were grown by recrystallization of crude product from hexane–diethyl ether (10 : 1) mixture. According to the SC XRD data, *p*-iminoquinone **2** crystallizes in the monoclinic space group $P2_1/c$ with the unique molecule in the asymmetric part of the unit cell. The dihedral angle between mean planes of the six-membered rings in **2** is 7.43(7)°. The bond lengths of C(1)=O(1) and C(2)–O(2) are 1.253(2) and 1.365(2) Å, respectively, with torsion angle OCCO equal to 4.4(2)°. In the *p*-iminoquinone six-membered cycle, a characteristic alternation of carbon bonds is observed: C(2)–C(3) [1.355(2) Å] and C(5)–C(6) [1.349(2) Å] bond lengths are significantly shorter than the others [1.442(2)–1.467(2) Å]. The C(4)=N(1) bond length is 1.324(2) Å, while the N(2)–N(1) [1.318(2) Å] and the N(2)–C(15) [1.404(2) Å] distances correspond to single bonds (Figure 1). Intramolecular short contact O(1)···H(2A) is realized in **2** with resulted distance 1.83(2) Å. Also, the intermolecular O···H interactions are detected in crystal packing of **2** with distances lying in the range 2.36(2)–2.60(2) Å. The shortest contact is O(1)···H(2B)–N(2) with O···N interatomic distance 3.120(2) Å.[†]

[†] *Crystal data for* **2**. $C_{20}H_{26}N_2O_2$, $M = 326.43$, $P2_1/c$, $a = 10.7302(7)$, $b = 14.6338(6)$ and $c = 12.5843(10)$ Å, $\beta = 109.764(5)°$, $V = 1859.63(12)$ Å^3, $Z = 4$, $d_{calc} = 1.166$ g cm^{-3}. Red single crystal with dimensions 0.58 × 0.31 × 0.28 mm was selected and intensities of 43772

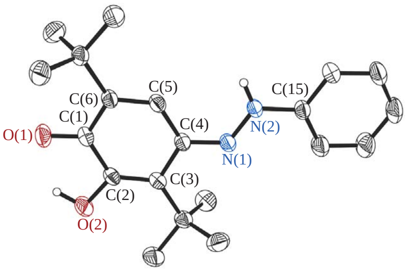

Figure 1 Molecular structure of **2**. Thermal ellipsoids are given at the 30% probability level. All hydrogen atoms except H(2A), H(2B) are omitted for clarity. For selected bond lengths and angles, see Online Supplementary Materials.

Obviously, the lifetime of azo-hydrazone tautomers in solution depends on several factors, including the nature of substituents in phenyl rings as well as the solvent used.[27] It was established that for the particular compound **2** combining phenyldiazenyl substituent and 3,6-di-*tert*-butylcatechol moiety, tautomeric equilibrium was truly observed in solution at room temperature (Scheme 2). ^{1}H NMR data recorded in several deuterated solvents show that there are two sets of proton peaks corresponding to both azo-catechol **2′** and quinone-hydrazone **2** tautomers. The key difference of ^{1}H NMR spectra for **2′** and **2** is in chemical shifts for their heteroatom-linked protons. In $CDCl_3$ both –OH protons of **2′** are located in the interval 5.0–6.5 ppm, that is typical for catechols.[28] As for **2**, it has a characteristic =N–NH hydrazone singlet with a chemical shift 8.76 ppm.

The relative concentrations of tautomers were calculated from the integral intensities of proton peaks assigned to their Bu^t groups. It was found that the ratio of tautomers varied slightly, depending on the solvent used (Table 1). In all cases, tautomer **2** was predominant, whereas the relative concentration of azo-catechol tautomer was the highest in non-polar solvents (31% in toluene, 33% in benzene).

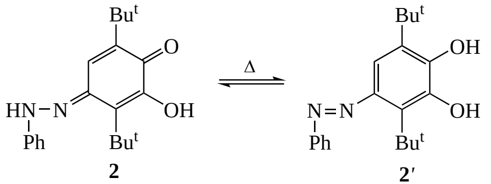

2 **2′**

Scheme 2

Table 1 Thermodynamic parameters of tautomerization.

Solvent	[**2′**] (%)^a	$K_{eq}{}^a$	ΔG_{298}/ kJ mol^{-1}	ΔH_T/ kJ mol^{-1}	ΔS_T/ J mol^{-1} K^{-1}
$CDCl_3$	24	0.30	2.98	9.3 ± 0.2	21.8 ± 0.7
Benzene-d$_6$	33	0.49	1.77	7.0 ± 0.2	17.5 ± 0.6
Toluene-d$_8$	31	0.45	1.97	7.7 ± 0.2	19.7 ± 0.9
CD_3CN	22	0.28	3.15	4.4 ± 0.2	3.2 ± 0.6

^{a}The data are given for 298 K.

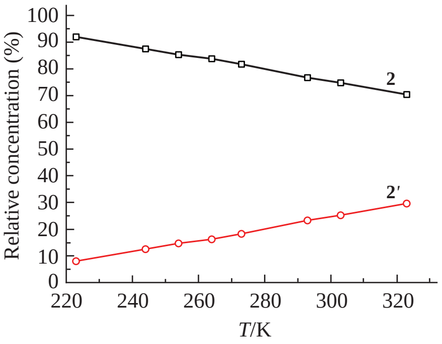

Figure 2 Relative concentrations of tautomers **2** and **2′** in $CDCl_3$ (C = 0.05 M) in the interval 223–323 K.

The temperature dependence of relative concentrations for tautomers **2′** and **2** in $CDCl_3$ was studied by ^{1}H NMR spectroscopy in the interval 223–323 K (Figure 2). It was established that at 298 K the ratio **2** : **2′** was equal to 76 : 24. When the sample was cooled to 223 K, the ratio changed to 92 : 8. ^{13}C NMR, recorded at 223 K, confirmed the structure of major **2** tautomer: at 323 K the ratio was 70 : 30. The same measurements were also carried out in toluene-d$_8$, and the **2** : **2′** ratio varied from 86 : 14 (223 K) to 63 : 37 (323 K). Maximum relative concentration of 41% for the minor tautomer **2′** was fixed in benzene-d$_6$ at 343 K.

Taking into account the value of azo–hydrazone equilibrium constant, calculated as K_{eq} = [**2′**]/[**2**], the temperature dependence of K_{eq} allowed us to evaluate thermodynamical parameters of isomerisation. The enthalpy and entropy values were extracted after linear fitting of lnK_{eq} *vs.* T^{-1} plots using the equation $\ln K_{eq} = -\Delta H/RT + \Delta S/R$. The obtained data are presented in Table 1.

Regardless of the solvent used, both ΔH and ΔS have the positive sign in the studied temperature interval and, therefore, their contribution to the thermodynamic free-energy difference between tautomers is opposite. The positive enthalpy favors the tautomer **2**, and such enthalpy difference may be tentatively attributed to the higher stabilization of hydrazone **2** with hydrogen bonds compared to **2′** tautomer. Although entropy contribution favors less polar azo-catechol **2′**, the enthalpy factor determines the free-energy difference between tautomers in the studied temperature interval. The obtained data correlate with that observed previously by Saeva for 4-[(*p*-methoxyphenyl)-diazenyl]-1-naphthol.[29]

In conclusion, it should be noted that reaction of 3-hydroxy-2,5-di-*tert*-butyl-1,4-benzoquinone with arylhydrazines may be regarded as an efficient synthesis of azo-substituted 3,6-di-*tert*-butylcatechols. The compounds thus prepared may serve as promising photoresponsive ligands for the synthesis of metal complexes exhibiting light-induced magnetic switching.

This work was supported by the Russian Science Foundation (grant no. 23-73-01250).

Online Supplementary Materials

Supplementary data associated with this article can be found in the online version at doi: 10.1016/j.mencom.2024.06.038.

---

reflections were collected (μ = 0.075 mm^{-1}, θ_{max} = 26.02°). After merging of equivalence and absorption corrections, 3664 independent reflections (R_{int} = 0.0356) were used for the structure solution and refinement. Final R factors R_1 = 0.0416 [for 2510 reflections with $F^2 > 2\sigma(F^2)$], wR^2 = 0.1206 (for all reflections), S = 1.003, largest diff. peak and hole are 0.14 and –0.13 e Å^{-3}, respectively. The SC XRD data for **2** was collected with Rigaku OD Xcalibur E diffractometer [MoK_α-radiation, ω-scans technique, λ = 0.71073 Å, T = 298.0(2) K] using CrysAlis^{Pro} software package.[24] Numerical absorption correction based on gaussian integration over a multifaceted crystal mode was performed. The structure was solved *via* intrinsic phasing algorithm and refined by full-matrix least squares on F^2 for all data using SHELX.[25,26] All non-hydrogen atoms were found from Fourier syntheses of electron density and refined anisotropically. All methyl hydrogen atoms were placed in calculated positions and refined isotropically with $U(H)_{iso} = 1.5\,U_{eq}$. The other hydrogen atoms were found from Fourier syntheses of electron density and refined isotropically. The thermal atomic displacement parameters of all atoms were restrained by RIGU instruction.

CCDC 2337803 contains the supplementary crystallographic data for this paper. These data can be obtained free of charge from The Cambridge Crystallographic Data Centre *via* http://www.ccdc.cam.ac.uk.

References

1 M. Natali and S. Giordani, *Chem. Soc. Rev.*, 2012, **41**, 4010.
2 D. Bléger and S. Hecht, *Angew. Chem., Int. Ed.*, 2015, **54**, 11338.
3 M. M. Khusniyarov, *Chem. – Eur. J.*, 2016, **22**, 15178.
4 H.-Y. Lin, Y.-T. Wang, X. Shi, H.-B. Yang and L. Xu, *Chem. Soc. Rev.*, 2023, **52**, 1129.
5 A. Beharry and G. A. Woolley, *Chem. Soc. Rev.*, 2011, **40**, 4422.
6 T. S. Zatsepin, L. A. Abrosimova, M. V. Monakhova, L. T. Hien, A. Pingoud, E. A. Kubareva and T. S. Oretskaya, *Russ. Chem. Rev.*, 2013, **82**, 942.
7 S. Crespi, N. A. Simeth and B. König, *Nat. Rev. Chem.*, 2019, **3**, 133.
8 M. N. Ryazantsev, D. M. Strashkov, D. M. Nikolaev, A. A. Shtyrov and M. S. Panov, *Russ. Chem. Rev.*, 2021, **90**, 868.
9 F. A. Jerca, V. V. Jerca and R. Hoogenboom, *Nat. Rev. Chem.*, 2022, **6**, 51.
10 O. Drath and C. Boskovic, *Coord. Chem. Rev.*, 2018, **375**, 256.
11 H.-J. Himmel, *Inorg. Chim. Acta*, 2018, **481**, 56.
12 A. Zolotukhin, M. P. Bubnov, V. K. Cherkasov and G. A. Abakumov, *Russ J. Coord. Chem.*, 2018, **44**, 272 (*Koord. Khim.*, 2018, **44**, 123).
13 T. Tezgerevska, K. G. Alley and C. Boskovic, *Coord. Chem. Rev.*, 2014, **268**, 23.
14 D. J. Harding, P. Harding and W. Phonsri, *Coord. Chem. Rev.*, 2016, **313**, 38.
15 M. Chegerev, O. Demidov, P. Vasilyev, N. Efimov, S. Kubrin, A. Starikov, V. Vlasenko, A. Piskunov, S. Shapovalova, A. Guda, Y. Rusalev and A. Soldatov, *Dalton Trans.*, 2022, **51**, 10909.
16 Y. Hasegawa, S. Kume and H. Nishihara, *Dalton Trans*., 2009, 280.
17 K.-P. Xie, Z.-Y. Ruan, B.-H. Lyu, X.-X. Chen, X.-W. Zhang, G.-Z. Huang, Y.-C. Chen, Z.-P. Ni and M.-L. Tong, *Angew. Chem., Int. Ed.*, 2021, **60**, 27144.
18 S. Venkataramani, U. Jana, M. Dommaschk, F. D. Sönnichsen, F. Tuczek and R. Herges, *Science*, 2011, **331**, 445.
19 S. Thies, H. Sell, C. Bornholdt, C. Schütt, F. Köhler, F. Tuczek and R. Herges, *Chem. – Eur. J.*, 2012, **18**, 16358.
20 K. Haghbeen and E. W. Tan, *J. Org. Chem.*, 1998, **63**, 4503.
21 H. F. Jirandehi and A. Mobinikhaledi, *Asian J. Chem.*, 2010, **22**, 6851.
22 L. I. Smith and W. B. Irwin, *J. Am. Chem. Soc.*, 1941, **63**, 1036.
23 A. Novikova, V. B. Vol’eva, N. L. Komissarova, I. S. Belostotskaya and V. V. Ershov, *Bull. Acad. Sci. USSR, Div. Chem. Sci.*, 1981, **30**, 1732 (*Izv. Akad. Nauk SSSR, Ser. Khim.*, 1981, 2110).
24 *Rigaku Oxford Diffraction, CrysAlisPro Software System, Version 1.171.40.67a*, Rigaku Corporation, Wroclaw, Poland, 2019.
25 G. M. Sheldrick, *Acta Crystallogr*., 2015, **A71**, 3.
26 G. M. Sheldrick, *Acta Crystallogr.*, 2015, **C71**, 3.
27 P. Ball and C. H. Nicholls, *Dyes Pigm*., 1982, **3**, 5.
28 T. N. Kocherova, N. O. Druzhkov, K. A. Martyanov, A. S. Shavyrin, M. V. Arsenyev, T. I. Kulikova, E. V. Baranov, V. A. Kuropatov and V. K. Cherkasov, *Russ. Chem. Bull.*, 2020, **69**, 2383.
29 F. Saeva, *J. Org. Chem.*, 1971, **36**, 3842.

Received: 15th March 2024; Com. 24/7426